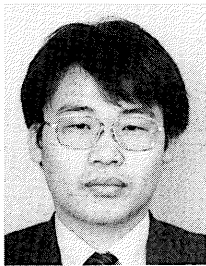
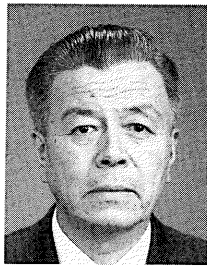


EVALUATION OF SHEAR STRENGTH OF RC BRIDGE PIERS USING
MODIFIED COMPRESSION FIELD THEORY

(Translation form Proceeding of JSCE, No. 620/V-43, May 1999)



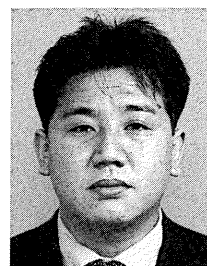
Kenji KOSA



Kazuo KOBAYASHI



Furitsu YASUDA



Takashi MIZUTA

To evaluate the shear strength of RC bridge piers, experiments were conducted using 1/3 scale specimens, an actual intact pier, and actual piers damaged by the Hyogoken-Nanbu Earthquake. The experimental results were compared with analytical results derived using the modified compression field theory. It was found that the analytical results were in relatively good agreement with the experimental results, which verified that the analytical procedure is usable for the shear strength evaluation of actual bridge piers.

According to the analysis, the shear resistance carried by the concrete gradually decreases once the main reinforcement yields until the maximum load is reached. Parametric studies also demonstrated that the greater the quantity of hoop ties, the greater the crack inclination angle, and that the 45° truss analogy tends to overestimate the shear resistance carried by the hoop ties.

Keywords: shear, Collins model, RC column, modified compression field theory

Kenji Kosa, a member of the JSCE and ASCE, is an associate professor in the Department of Civil Engineering at the Kyushu Institute of Technology. Before joining the faculty in 1999, he was a senior highway engineer at the Hanshin Expressway Public Corporation in Osaka. He obtained his Ph.D. from the University of Michigan in 1988. His main research interests are the design and analysis of concrete structures.

Kazuo Kobayashi is a professor in the Department of Civil Engineering at the Osaka Institute of Technology, Osaka, Japan. He received his Dr. Eng. from Kyoto University in 1973. He has authored several books and numerous papers on the behavior and analysis of reinforced and prestressed concrete structures. He is a fellow of the JSCE.

Furitsu Yasuda is a senior highway engineer at the Hanshin Expressway Public Corporation in Osaka. He obtained his Dr. Eng. from Osaka University in 2000. His research interest is the seismic design of concrete structures. He is a member of the JSCE and JGS.

Takashi Mizuta is a structural engineer at the Kansai Branch of Oriental Consultants Co. Ltd. He obtained his MS in civil engineering from Ritsumeikan University in 1995. His research interest is the design of concrete structures. He is a member of the JSCE.

1. INTRODUCTION

Approximately 600 out of 1,100 RC piers along the Hanshin Expressway Kobe Route suffered damage of varying degrees during the Hyogoken-Nanbu Earthquake of 1995. Damage to the piers was predominantly due to flexure or flexural shear, and though few piers were damaged by shear, the damage was very significant. Incidentally, the piers damaged by flexural shear can also be grouped into the shear damaged category, because that type of damage occurs as a result of a member that has already suffered cracks losing its shear resistance under continued reversed cyclic loading. Unlike flexural damage, shear damage is often dangerous as it may result in brittle fracture. To prevent this and establish an adequate design procedure, a proper understanding of the shear mechanism of RC bridge piers is urgently needed.

The shear strength of RC structures is determined by a complicated interaction of factors such as the main reinforcement ratio, concrete strength, hoop tie ratio, and the size and shape of the cross section. Because of this complexity, empirical laws obtained through experiments have conventionally been used for evaluation of the strength of RC structures. Recently, however, as computer technology has developed, attempts to evaluate the ultimate shear strength of structures through analysis have been increasing. One such attempt is a procedure based on the "Modified Compression Field Theory" proposed by Collins et al.^{1) 2)} Modified compression field theory does not assume that cracks in the concrete are separate entities, but treats them as a sort of sequential element from a macroscopic standpoint. Analysis relies on the equilibrium and compatibility conditions within the element relative to the average stress and average strain. This method enables the shear stress of members and crack inclination angle to be derived relatively easily.

It is known that the spacing of main reinforcement and hoop ties in actual piers is wider than in experimental specimens, and that the interlocking effect of aggregate particles in actual piers is smaller than in specimens due to the relative size difference of aggregates and the column cross section. As a result, the shear strength of actual piers is comparatively lower than that of specimens. Nevertheless, there is still a shortage of investigations aimed at evaluating the shear strength of actual bridge piers both by experiment and analysis.

The authors attempt to evaluate the shear failure mechanism of actual bridges using experimental results and analytical results obtained through the Collins Model, as follows: first, using two 1/3 scale RC specimens and an actual intact RC pier, the shear strength, crack inclination angle, and hoop tie stress are evaluated experimentally and analytically. Next, using five actual piers which sustained considerable shear damage during the Hyogoken-Nanbu Earthquake, the shear strength, damage pattern, and crack inclination angle are evaluated. Lastly, by conducting parameter analysis using these analytical results, the possible effect of these pier characteristics on the shear strength and crack inclination angle of piers is evaluated.

2. ANALYTICAL PROCEDURE

2.1 Basics of Modified Compression Field Theory

The analysis described in this study was conducted using the Modified Compression Field Theory, as proposed by Collins et al. in Reference 3). An outline of this theory is given here.

The horizontal strain and vertical strain (ϵ_x , ϵ_y) and principal tensile strain and principal compressive strain (ϵ_1 , ϵ_2) have the following relationship based on Mohr's stress circle:

$$\epsilon_x = (\epsilon_1 \tan^2 \theta + \epsilon_2) / (1 + \tan^2 \theta) \quad \dots\dots\dots (1)$$

$$\epsilon_y = (\epsilon_1 + \epsilon_2 \tan^2 \theta) / (1 + \tan^2 \theta) \quad \dots\dots\dots (2)$$

The average principal tensile stress, f_t , and the average principal compressive stress, f_c , acting on a concrete plane with shear cracks have the following relationship based on Mohr's stress circle (Fig. 1):

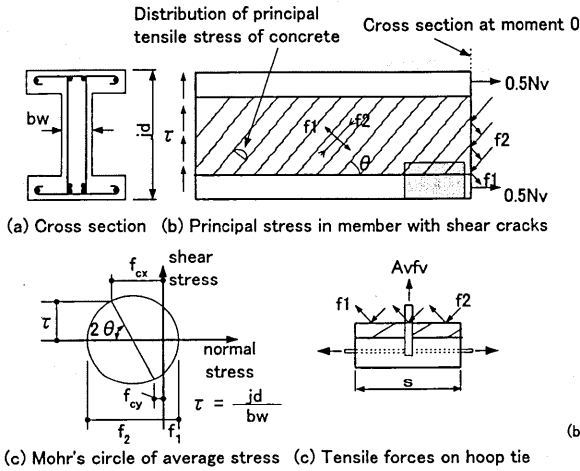


Fig. 1 Stresses assumed in the Modified Field Compression Theory

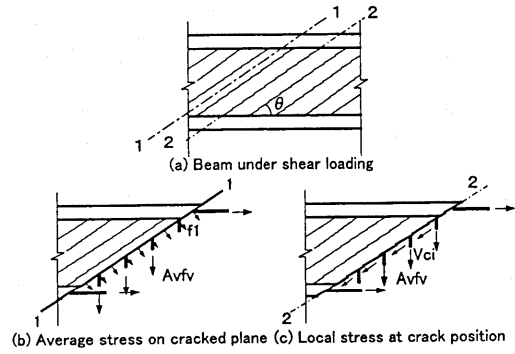


Fig. 2 Transfer of force via cracked plane

$$f_2 = (\tan \theta + \cot \theta) v - f_1 \quad \dots \quad (3)$$

Where,

θ : angle formed by f_2 and the member axis (shear crack inclination angle)

v : shear stress ($v = V/(b_w j d)$)

V : shear force

b_w : width of web

$j d$: arm length of the couple of resisting forces

When the cross sectional area of hoop ties is A_v , the spacing s , and the stress f_v , the following equation is derived from an equilibrium requirement of forces in the vertical direction, as shown in Fig. 1:

$$A_v f_v = (f_2 \sin^2 \theta - f_1 \cos^2 \theta) b_w s \quad \dots \quad (4)$$

or, if expressed in terms of hoop tie stress, the equation is as follows:

$$f_v = (f_2 \sin^2 \theta - f_1 \cos^2 \theta) b_w s / A_v \quad \dots \quad (5)$$

If f_2 in Equation (3) is substituted for Equation (4), then

$$V = f_1 \cdot b_w \cdot j d \cdot \cot \theta + (f_v \cdot A_v / s) \cdot j d \cdot \cot \theta \quad \dots \quad (6)$$

Equation (6) indicates that the shear strength of the member can be expressed as the sum of the shear resistance carried by the concrete and the shear resistance carried by the hoop ties.

In Fig. 1, the axial force (internal force), N_v , derived by the following equation based on the equilibrium of forces in the horizontal direction, must be resisted by the longitudinal reinforcement, $A_{sx} F_{sx}$ (A_{sx} , F_{sx} : cross sectional area and stress of longitudinal reinforcement, respectively).

$$N_v = (f_2 \cos^2 \theta - f_1 \sin^2 \theta) b_w j d \quad \dots \quad (7)$$

From equations (3) and (7), the following equation is derived:

$$N_v = V \cot \theta - f_1 b_w j d \quad \dots \quad (8)$$

To express the relationship between the principal compressive stress, f_2 , and principal compressive strain, ϵ_2 , of the concrete, the following equations proposed by Vecchio & Collins are used:

$$f_2 = f_{2max} [2 (\epsilon_2 / \epsilon'_c) - (\epsilon_2 / \epsilon'_c)^2] \quad \dots \quad (9)$$

$$f_{2max} / f'_c = 1 / (0.8 + 170 \epsilon_1) \leq 1.0 \quad \dots \quad (10)$$

Where, f'_c = unconfined compressive strength of the concrete.

On the other hand, to express the relationship between the average principal tensile stress, f_1 , and the average principal tensile strain, ϵ_1 , of the cracked plane, the following equations proposed by Vecchio & Collins (which take tension stiffening into account) are used:

$$f_1 = E_c \epsilon_1 \quad (0 \leq \epsilon_1 < \epsilon_{cr}) \quad \dots\dots\dots (11)$$

$$f_1 = f_{cr} / (1 + \sqrt{500 \cdot \epsilon_1}) \quad (\epsilon_{cr} \leq \epsilon_1) \quad \dots\dots\dots (12)$$

From the following equation (Equation 13), which means that the shear force transmitted across the cracks is equivalent to the shear force transferred via a plane with cracks, the upper value of f_1 is expressed by Equation (14) (Fig. 2).

$$A_v f_v (jd / s \cdot \tan \theta) + f_1 b_w jd \cdot \cos \theta / \sin \theta = A_v f_{vy} (jd / (s \cdot \tan \theta)) + V_{ci} b_w jd \quad \dots\dots\dots (13)$$

$$f_1 = V_{ci} \cdot \tan \theta + A_v (f_{vy} - f_v) / (s \cdot b_w) \quad \dots\dots\dots (14)$$

Where,

f_{vy} : yield strength of hoop ties

v_{ci} : shear stress transferred via crack interface of the concrete.

Collins et al. use the following equation for v_{ci} :

$$v_{ci} = 0.18 \cdot \sqrt{f_c} / (0.3 + 24w / (a + 16)) \quad (\text{MPa, mm}) \quad \dots\dots\dots (15)$$

Where,

a : maximum aggregate size

w : shear crack width

In Equation (15), 'w' can be expressed as the product of ϵ_1 and the average shear crack spacing, $s_{m\theta}$, as follows:

$$w = \epsilon_1 \cdot s_{m\theta} \\ s_{m\theta} = 1 / (\sin \theta / s_{mx} + \cos \theta / s_{mv}) \quad \dots\dots\dots (16)$$

Where,

s_{mx} : average crack spacing in the longitudinal direction

s_{mv} : average crack spacing in the transverse direction.

Collins et al. use the equations recommended in the CEB-FIP Model Code (1990) for s_{mx} and s_{mv} in Equation (16).

The tensile force of the concrete which would be transferable, is restricted due to yielding of the longitudinal reinforcement. In order for the horizontal forces generated by the average stress of the cracked plane and by the local stress of the cracked plane to be equal, the following equation must be satisfied (Fig. 2):

$$A_{sx} f_y \geq A_{sx} f_{sx} + f_1 b_w jd + [f_1 - A_v (f_{vy} - f_v) / (b_w s)] \cdot b_w jd \cdot \cot^2 \theta \quad \dots\dots\dots (17)$$

2.2 Simplification under Combined Shear, Flexure, and Axial Forces

Usually, the shear force (V) does not act alone, but acts with a combination of bending moment (M) and axial force (N). Consequently, stress and strain vary in the longitudinal direction of the column, but a detailed analysis of this phenomenon takes an enormous amount of time. Accordingly, Collins et al. attempt to simplify the process as follows (Fig. 3):

- ① Ignore the redistribution of shear stress in the high-load region, and assume that shear stress is distributed uniformly over the cross section of the column ($v = V/b_w jd$), and that shear cracks occur throughout the entire web height.
- ② Calculate a shear crack inclination angle, θ , at a specific point on cross section, and assume that the value is uniform in the direction of the web height.

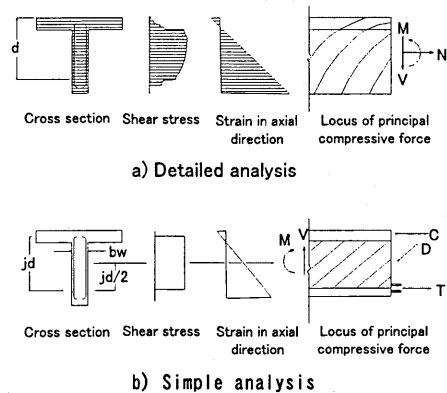


Fig. 3 Analysis under shear, flexure, and axial force

In actual analysis, the cross section is divided into a shear analysis region (the web) and a flexural analysis region (region other than the web), and then the modified compression field theory is applied to the former and bending theory to the latter.

2.3 Calculation

Calculations are repeated according to the flowchart shown in Fig. 4 until reaching convergence. In this analysis, the "section-dividing" method is used, in which the cross section is divided into a number of elements in the longitudinal direction for applicability to any cross sectional shape to calculate the equilibrium of flexure, shear, and axial forces according to Fig. 4. The horizontal force is applied at the centroid of the superstructure as regards the bridge axis direction and at the top of the substructure in the direction perpendicular to the bridge axis in the case of actual bridge piers, and at the loading point in the case of specimens. The shear span of actual bridge piers is taken as the distance from the inertia force-acting point on the superstructure (bridge axis direction: centroid of the superstructure; perpendicular direction: top of the substructure) to the point at which critical shear cracks intersect with the member axis. The shear span of the specimens is made the distance from the horizontal force-loading point to the point at which shear cracks intersect with the member axis.

Some have said that many of the actual piers along the Kobe Route that had already been subjected to reversed cyclic earthquake loading are not really suitable for evaluation by the Collins model which is basically intended for one directional loading. However, it can be responded that such piers can be evaluated by this model because, if the strain of the longitudinal reinforcement remains approximately within three times the yield strain, the effect of the earthquake loading was slight⁴⁾. The piers under investigation have a small hoop tie ratio and the analytical values of longitudinal reinforcement strain at yielding of the hoop ties (ultimate state) are less than three times the yield strain in all except Specimen 2, which is explained later, and accordingly it is concluded that the piers can be qualitatively evaluated by the Collins model. Experimental and analytical results derived from 1/3 scale specimens, an actual pier without damage, and actual piers damaged by the Hyogoken-Nanbu Earthquake are presented in the following section.

3. EXPERIMENT WITH 1/3 SCALE SPECIMENS

Two 1/3 scale specimens modeling the reinforcement details of standard piers on the Hanshin Expressway, as designed by the Specifications of Highway Bridges of 1990, were constructed (Specimens 2 and 3). As is conventional, one 1/10 scale specimen was also made for comparison (Specimen 1). Specimens 1 and 2 were constructed to be base-failure types. Specimen 3 was built as a flexural failure type, designed to fail at the point of reinforcement termination. They were loaded and their flexural capacity and shear strength were evaluated.

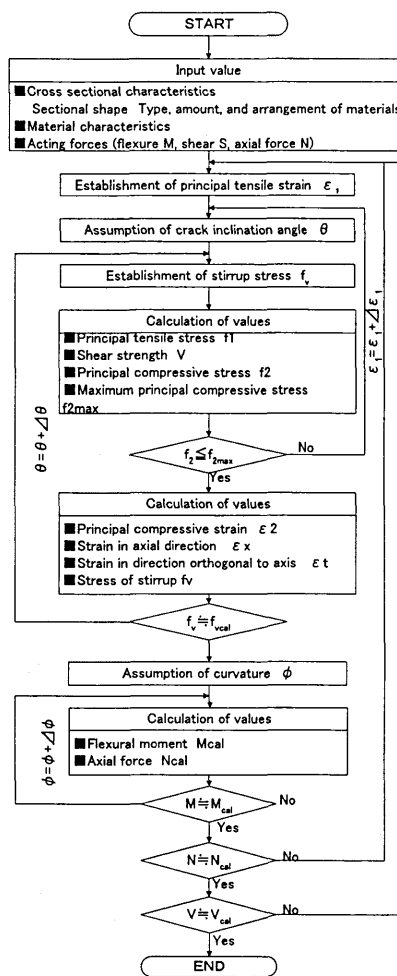


Fig. 4 Calculation flowchart

Applying the Collins model to the experimental results, the shear damage mechanism of the bridge piers was investigated. Details of the experimental procedure are presented in Reference 5 (the objective of investigation in this reference was the flexural deformation characteristics of Specimens 1 and 2. The loading method was the same for Specimen 3), and only an outline is given here. The experimental attributes of each specimen are shown in Table 1. D13 reinforcement was used for Specimens 2 and 3 so that scaling of reinforcement diameter was close to that of Specimen 1. The amount of reinforcement in each specimen was determined so as to obtain a similar ratio between the cross sectional area of the specimen and the area of reinforcement. The test setup is shown in Fig. 5. Horizontal force was applied to the specimen in a reverse loading manner, while axial force was applied to the column top. An axial force equivalent to an axial stress of 15kgf/cm^2 was applied using a jack attached to the column top via PC steel bars encased in the column center and anchored at the footing bottom.

Loading was applied by the load-control method up to the calculated yield load, P_y , the load at which the longitudinal reinforcement in the outermost layer at the column bottom reaches the yielding point. After reaching the yield load, ten cycles of reversed load were applied at each multiple of yield-load displacement (δ_y). Specimens 1 and 2 failed at the column bottom and exhibited desirable deformational characteristics with a ductility factor of $5 \sim 6$. In Specimen 3, the longitudinal reinforcement yielded and then failed at the point of reinforcement termination. Though both the maximum load and ductility factor of this specimen were lower compared with those of Specimen 2, a ductility factor of 4 was duly secured and brittle failure mode was not indicated.

Table 1 Experimental attributes of specimens

Specimen	Scale	Main reinforcement arr	Termination of rebars	Hoop tie arr	Max. size of coarse aggregate
NO.1	1/10	One layer D16	None	Closed D16	20mm
NO.2	1/3	Multi-layers D13	Standard position	Not closed D16	20mm
NO.3	1/3	Multi-layers D13	*1 1 d lower	Not closed D16	20mm

*1 d: effective height of cross section

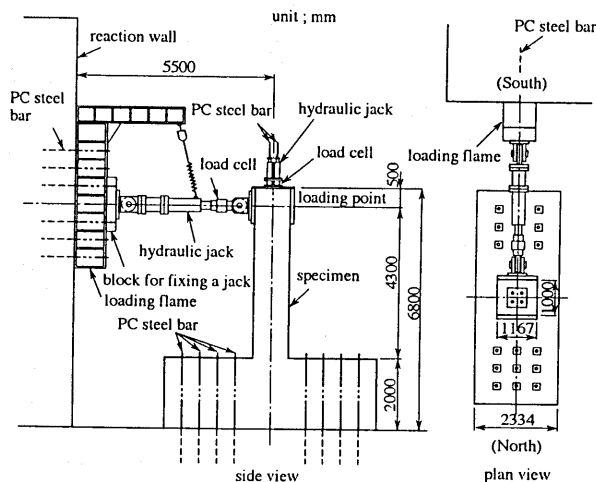


Fig. 5 Dimensions of the specimen and loading method (Large size model)

4. ANALYTICAL RESULTS FOR 1/3 SCALE SPECIMENS

4.1 Results for Specimen 1

Figure 6 shows the relationship between hoop tie stress (at a position 10 cm from the column bottom) and shear force. Calculated hoop tie stress was 750 kgf/cm^2 at the longitudinal reinforcement yield point (8.13 tf) and $3,300 \text{ kgf/cm}^2$ at the maximum load (11.2 tf), while the measured stress at the maximum load was $1650 \sim 2450 \text{ kgf/cm}^2$, indicating a qualitative agreement in terms of the correlation between rise in hoop tie stress and load increase. Failure of Specimen 1 occurred at a section $0.8d$ from the column bottom (d : effective depth of cross section; 35 cm for Specimen 1) where shear cracks were especially conspicuous. The average inclination angle of the cracks observed at the end of testing was 60° . The analytical value of crack inclination angle at a point 10 cm from the column bottom was 59° . The analytical hoop tie stress may vary according to position on the column because it takes into account the coupling of flexure and shear, but the analytical value at a point 10 cm from the column bottom was roughly equal to the average measured value at the same position.

4.2 Results for Specimen 2

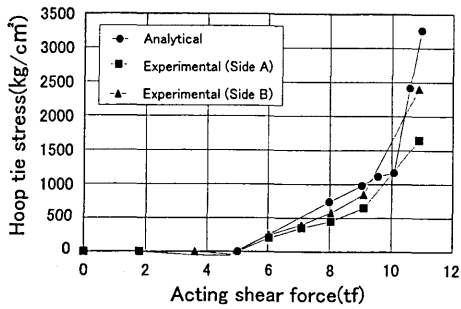
Figure 7 shows the relationship between hoop tie stress (at a position 216 cm from the column bottom) and shear force. Calculated hoop tie stress varied from 50 kgf/cm^2 at the yield load (90.3 tf) to $2,500 \text{ kgf/cm}^2$ at the maximum load (122.0 tf). The crack inclination angle at the maximum load was 65° by measurement and 59° by analysis. The failure mode of this specimen was governed by flexure as with Specimen 1, but, it is inferred from the experimental and analytical results that the acting shear force also came close to the ultimate shear strength. From Fig. 7, it is seen that analytical hoop tie stress progresses gradually, while experimental values rise slowly at first before abruptly increasing around the ultimate load. This tendency was also observed in Specimen 3, and is probably because in the analysis cracks are assumed to disperse and progress uniformly, whereas in actual piers they do not disperse very steadily and some cracks suddenly begin propagating as the load accumulates.

4.3 Results for Specimen 3

Specimen 3 exhibited yielding of hoop ties at the point of reinforcement termination and fracture occurred at the same point. Figure 8 shows the relationship between hoop tie stress (at a position 123 cm from the bottom) and shear force. Experimental hoop tie stress was $300 \sim 400 \text{ kgf/cm}^2$ at the time of yield loading and $1,800 \sim 3,000 \text{ kgf/cm}^2$ at the maximum load. Analytical hoop tie stress was 100 kgf/cm^2 at yield loading (75.2 tf) and $1,250 \text{ kgf/cm}^2$ at the maximum load (105.0 tf), indicating a fairly good qualitative agreement with the experimental values. The crack inclination angle was 50° at the end of experiment, but was 60° by analysis, as shown in Fig. 9. The shear strength by analysis was approximately 130 tf, an excess of nearly 25 tf over the experimental results. This was probably because, in the experiment, shear strength saw a further decrease due to reversed cyclic loading applied at the point of reinforcement termination, while in the analysis, the evaluation method entailed calculating the stress transferred via a shear crack plane, as indicated below.

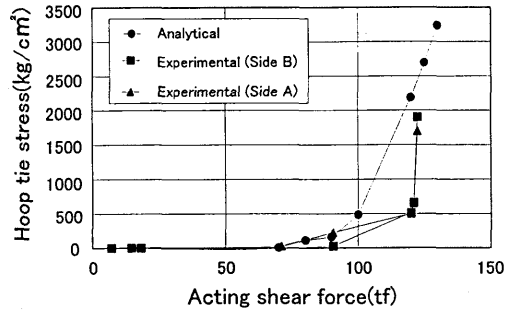
Figure 10 shows the relationship between acting shear force and shear resistance of the concrete and the shear reinforcement, as derived by analysis. At the initial stage, the concrete accounts for the majority of shear resistance, but as the hoop tie stress increases, the proportion carried by the concrete gradually drops. This tendency is seen in all three specimens, but it is inconsistent with the cumulative equation given in the Concrete Specifications. This inconsistency can be explained using Fig. 11, which shows the relationship between the principal tensile stress and principal tensile strain derived by the Collins model. Range I in the figure is where the principal tensile stress of the concrete is still elastic, and it extends up to an acting force of 70 tf in the case of Specimen 3. Range II is that governed by the tensile-softening curve (Equation 12) and extends up to 100 tf, at which the shear resistance of the concrete reaches the maximum. In Range III, the shear stress is governed by the principal tensile stress (Equation 14), which is

transferred via the shear crack plane. Here, the shear resistance of the concrete abruptly decreases as shown in Fig. 11. In accordance with this, the crack inclination angle undergoes a change and the shear resistance accounted for by the hoop ties suddenly increases. As is clear, the shear behavior in this range exhibits a conspicuous change. Because of this and also the fact that the stress-strain relationship in this range has a major effect on the ultimate shear strength, this range needs to be studied further using a constitutive law of higher precision.



* Sides A and B represent the sides of the loaded plane

Fig. 6 Relationship between hoop tie stress and acting shear force (Specimen 1)



* Sides A and B represent the sides of the loaded plane

Fig. 7 Relationship between hoop tie stress and acting shear force (Specimen 2)

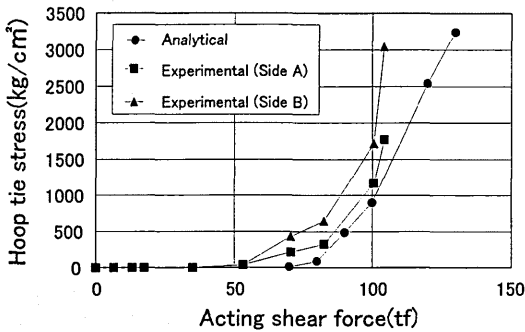


Fig. 8 Relationship between hoop tie stress and acting shear force (Specimen 3)

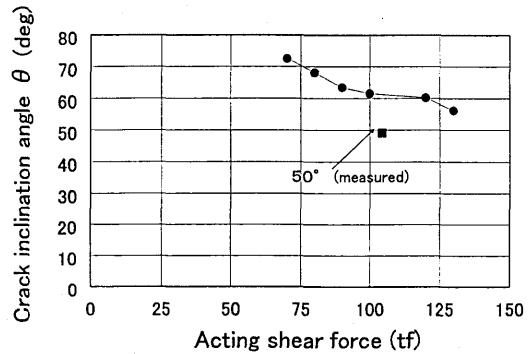


Fig. 9 Acting shear force vs. crack inclination angle (Specimen 3)

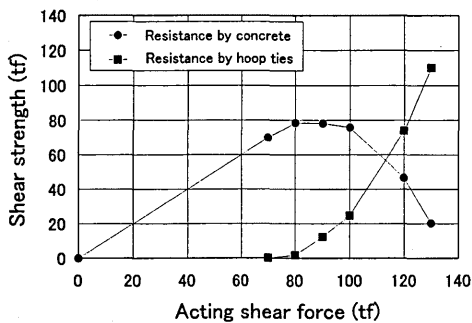


Fig. 10 Relationship between acting shear force and shear resistance (Specimen 3)

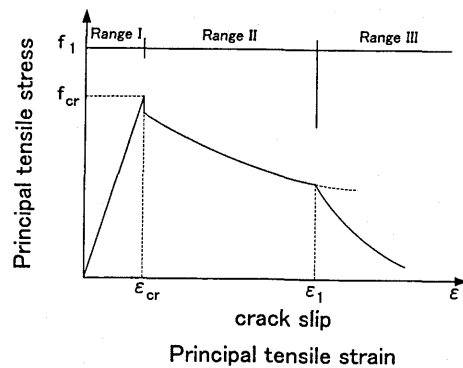


Fig. 11 Relationship between principal tensile stress and principal tensile strain

5. HORIZONTAL LOAD APPLICATION TO ACTUAL INTACT PIER

5.1 Structural Details

After removing the existing superstructure, the top of an actual bridge pier (URP4) was linked horizontally to the top of a reaction pier (URP3) by means of a PC steel bar. A horizontal load was applied such that the two piers were drawn toward each other, as shown in Fig. 12. The pier tested was an RC single pier with a circular cross section of ϕ 2.0 m, and the foundation was made of cast-in-place piles (ϕ 1.0 m) driven by the Benoto method, as shown in Fig. 13. The main reinforcement arranged in the column consisted of 53 D29 reinforcing bars at the column bottom and 28 D29 bars at the point of reinforcement termination. The longitudinal reinforcement ratio at the column bottom was 1.62%.

The pier was constructed in 1965 according to the Specifications for Steel Highway Bridges of the time. When compared with today's Specifications for Highway Bridges, it differs in the following respects: the point of reinforcement termination at the time was 2.7 m from the column bottom, but it is 1.7 m from the column bottom nowadays because a reinforcement anchoring length of 30ϕ is assumed. A calculation based on current standards indicates that this pier would fail at the point of reinforcement termination rather than at the column bottom. The spacing of D16 hoop ties in the pier is as sparse as 300 mm. The concrete compressive strength of the pier as determined by a core test was approximately 50 ~ 60% higher after 30 years in service compared with the 240 kgf/cm² of the original design. The yield stress of the pier reinforcement was 3,800 kgf/cm², which was considerably larger than the 2,800 kgf/cm² of the original design.

5.2 Loading Method

The horizontal load application point (the centroid of the PC steel bar) was made the mid-point of beam height (1.3 m) on pier URP4, and the PC steel bar was extended horizontally to the reaction pier, URP3. Loading was applied in a cyclic cumulative manner by increasing the load by 15 tf up to the fifth step, and at the sixth step the maximum load was applied.

5.3 Experimental Results

Up to the fifth loading step (75 tf), no evident damage was observed except for some flexural cracks around the column bottom. From around a load of 100 tf, column deformation began to be observed visually and horizontal cracks around the point of reinforcement termination became gradually obvious. As the load increased, these horizontal cracks started to progress toward the lower bottom. When the cracks reached the column bottom (133 tf), the column was no longer able to sustain the load, leading to the ultimate point. The residual maximum crack width was approximately 10 mm.

As shown in Fig. 14, flexural cracks occurred horizontally in the column at intervals of about 50 cm, a little wider than the hoop tie spacing of 30 cm. It is clear from the load-displacement relationship in Fig. 16 that a point around 3 m from the bottom, at which the horizontal displacement increases sharply (the bend point), corresponds to the point of reinforcement termination.

As shown in Fig. 17, hoop tie strain around the point of reinforcement termination was not evident up to 120 tf, but after this load a marked increase in strain was observed. Concrete strain on the compressive side and longitudinal reinforcement strain on the tensile side were most evident around the point of reinforcement termination rather than the column bottom. The former reached 1,900 μ and the latter well exceeded the yield strain ($\epsilon_{sy} = 1800 \mu$) derived from material strength tests (for which figures are not included). Thus, the test pier was judged to have failed by flexural shear in view of an increase in hoop tie strain and crack inclination angle at the ultimate point, though this was preceded by flexural cracks.

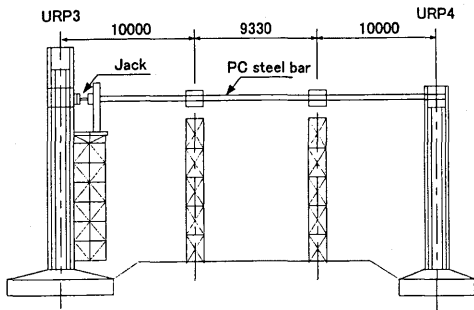


Fig. 12 Loading of actual intact pier

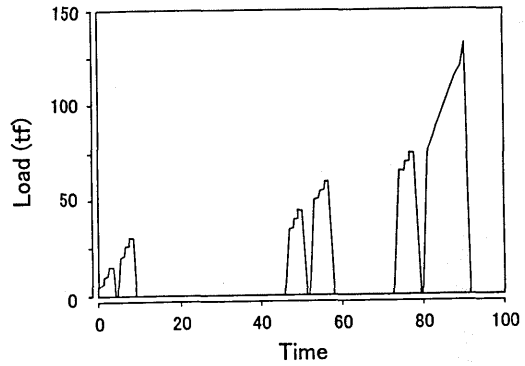


Fig. 15 Loading steps

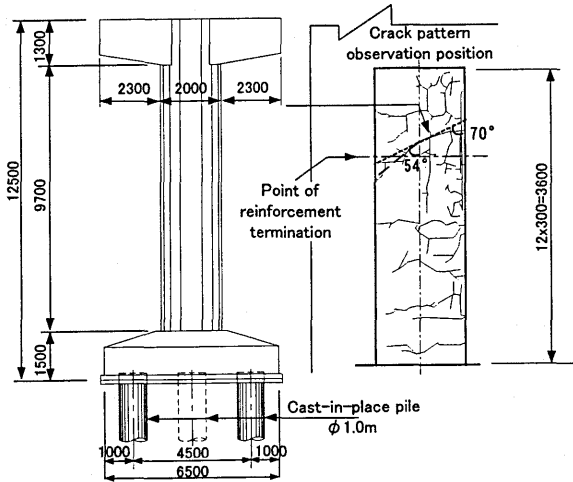


Fig. 13 General structure Fig. 14 Cracking pattern

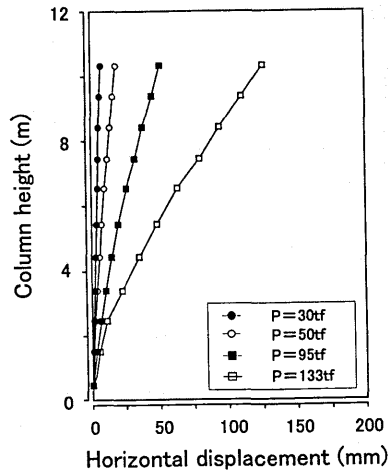


Fig. 16 Load-displacement relationship

5.4 Results of Analysis

Experimental and analytical results are compared in Figs. 17 and 18, indicating a relatively good agreement. When the load was at its maximum (133 tf), the hoop tie stress and crack inclination angle derived by analysis were 1,740 kgf/cm² and 57°, respectively, whereas the values by experiment were 2,700 kgf/cm² and 70°. The load derived by analysis at the time of shear crack appearance was 100 tf, which is roughly in correspondence with the load obtained by experiment (110 tf) and that given by the Concrete Specifications (110 tf).

In contrast, the shear strength derived by analysis at the ultimate point was 150 tf, considerably smaller than that given by the Concrete Specifications (177 tf). As shown in Fig. 18, the experiment reached the ultimate point when the crack inclination angle was 70° and the maximum load was 133 tf. But according to analysis using the Collins model, approximately 20 tf of strength remained, and the crack inclination angle decreased after the column reached the ultimate point. In this analysis, the Collins model was used to evaluate the shear resistance behavior of an actual bridge pier with a circular cross section. Because of experimental constraints, the ultimate strength and the ultimate behavior of the column were not pursued experimentally, but it was verified that the behavior up to a point near the ultimate point can be evaluated using the Collins model, although a further enhancement in analytical precision may be needed.

6. ANALYSIS OF PIERS DAMAGED BY EARTHQUAKE

6.1 Overview

Analysis was conducted on actual piers damaged by the 1995 Hyogoken-Nanbu Earthquake to evaluate their shear resistance behavior. Five piers selected in a parametric study were subjected to analysis, but only two that represent shear damage and flexural shear damage, respectively, are presented here. The focus was on a cross section located centrally among the dominant cracks in the column.

6.2 Pier Damaged by Shear (P270)

This pier is an RC single pier with a rectangular cross section measuring 4.2 m (bridge axis direction) x 3.5 m (perpendicular direction), and the longitudinal reinforcement is not terminated. The longitudinal reinforcement consists of D32 reinforcing bars, and the D16 hoop ties are arranged at a spacing of 25 cm. The pier was damaged in the bridge axis direction, as shown in Fig. 20. Shear cracks occurred around the column center and propagated toward the lower bottom at an acute angle of nearly 30° . Neither spalling of the cover concrete nor buckling of the longitudinal reinforcement was observed.

6.3 Analytical Results for Pier Damaged by Shear (P270)

The cross section at the position where the cracks intersect with the centerline of the column (shear span: 6 m) are studied. The analytical results of the bridge axis direction of this cross section are shown in Figs. 21 and 22. The crack inclination angle observed in the actual pier (30°) was in good agreement with the crack inclination angle (30°) at the time of hoop tie

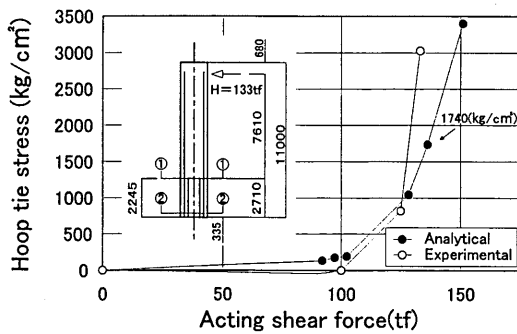


Fig. 17 Hoop tie stress vs. acting shear force (cross section ①-①)

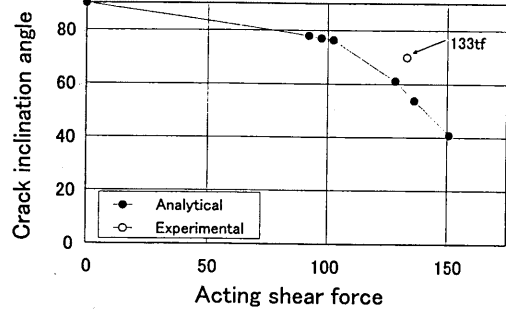


Fig. 18 Acting shear force vs. crack inclination angle

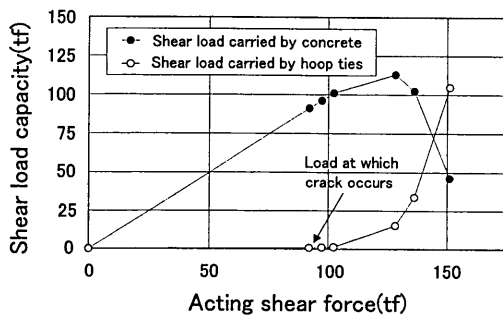


Fig. 19 Shear load carried by concrete and hoop ties

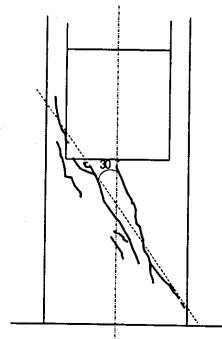


Fig. 20 Shear damage on actual pier

yielding ($3,000 \text{ kgf/cm}^2$) derived by analysis using the Collins model, as shown in Fig. 21. The calculated stress of the longitudinal reinforcement at that time was a rather small value of 855 kgf/cm^2 , which remains in the elastic range. From this, it can be assumed that damage was predominantly governed by shear, not by flexure.

The shear strength calculated in accordance with the Concrete Specifications is also included in Fig. 22. The shear force carried by the concrete at the ultimate state was 335 tf and 387 tf, respectively, by analysis and according to the equation in the Concrete Specifications. Thus, the analytical value was smaller than the value given by the Concrete Specifications, though the contrary was true when the shear strength carried by the hoop ties was calculated. Then, the analytical value (315 tf) was larger than the value given by the Concrete Specifications (192 tf), because the crack inclination angle was small in the analysis. The combined shear force carried by the concrete and the hoop ties was 650 tf by analysis using the Collins model and 579 tf by the Concrete Specifications, the former approximately 10% larger than the latter.

6.4 Pier Damaged by Flexural Shear (P227)

Damage to this pier is shown in Fig. 23. The longitudinal reinforcement buckled primarily in the direction perpendicular to the bridge axis, the cover concrete spalled on all four sides, and the inclination angle of shear cracks was about 40° . Damage was presumed to be the combined flexural-shear triggered by a decline in the shear strength of the concrete due to continued reversed cyclic loading after the flexural cracks formed.

6.5 Analytical Results for Pier Damaged by Flexural Shear (P227)

The cross section at the point where the cracks intersect with the centerline of the column (shear span: 7 m) was adopted as the cross section for analysis. The analytical results obtained from the direction perpendicular to the bridge axis of this cross section are shown in Figs. 24 and 25. It is seen in Fig. 24 that hoop tie stress appears when the acting shear force is 250 tf, and suddenly increases from around 350 tf. The shear force carried by the concrete increased uniformly up to an acting shear force of 350 tf, where it reached a maximum, but then suddenly dropped. From around this maximum, the shear force carried by the hoop ties suddenly rose. As seen in Fig. 23, the crack inclination angle was approximately 40° . At the time of this crack inclination angle, the analytical shear strength is about 420 tf ($V_c = 310 \text{ tf}$, $V_s = 110 \text{ tf}$) from Figs. 24 and 25 and the hoop tie stress about $2,500 \text{ kgf/cm}^2$.

Judging from the ultimate crack inclination angle of the actual pier, the hoop tie stress was within the range that exhibits an abrupt increase with rising shear force, but it had not yet reached the yield strength ($\sigma_{sy} = 3,000 \text{ kgf/cm}^2$). Analytically, it was probably at a point very close to shear failure.

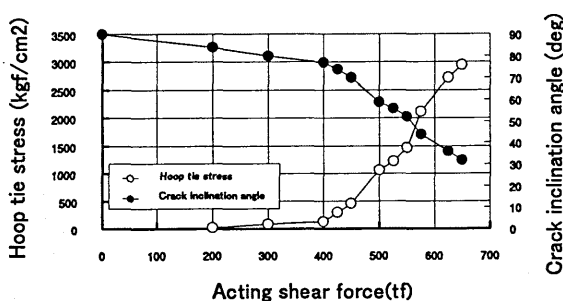


Fig. 21 Relationship between crack inclination angle/hoop tie stress and shear force

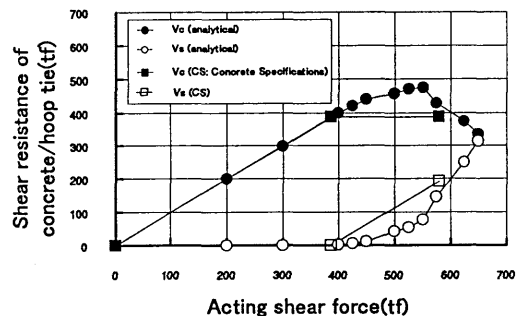


Fig. 22 Relationship between V_c/V_s and acting shear force

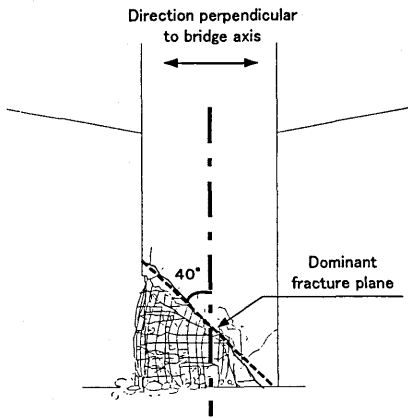


Fig. 23 Damage to Pier P227

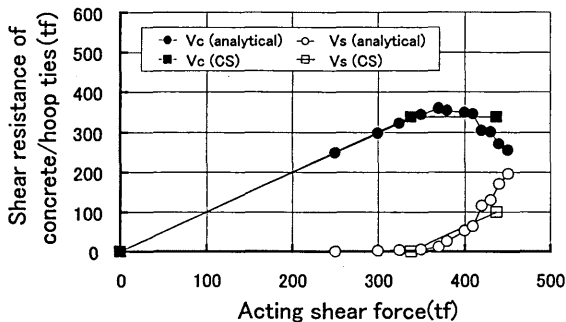


Fig. 24 Relationship between V_c/V_s and acting shear force

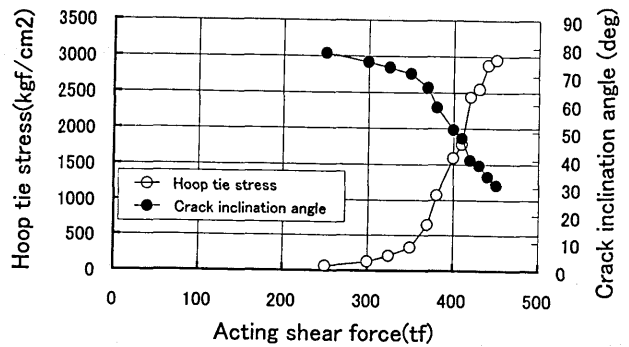


Fig. 25 Relationship between crack inclination angle/hoop tie stress and acting shear force

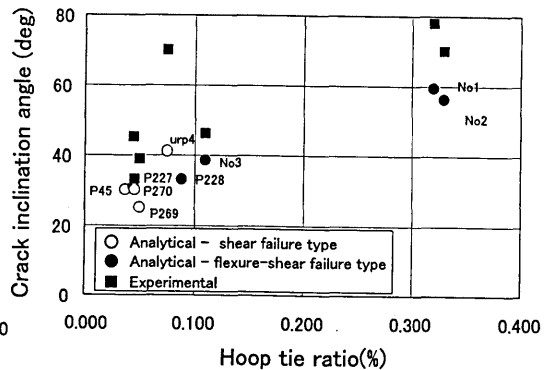


Fig. 26 Relationship between crack inclination angle and hoop tie ratio

7. PARAMETER ANALYSIS USING THE COLLINS MODEL

7.1 Piers for Parameter Analysis

A total of nine piers, the six piers cited so far (including the three scale specimens) plus the following three damaged by the Hyogoken-Nanbu Earthquake, were chosen for parameter analysis. Two of these latter three piers, P45 and P269, were damaged mainly by shear, and the remaining one, P228, was damaged by flexural shear.

7.2 Crack Inclination Angle

Factors that influence the shear crack inclination angle at the ultimate state include the tensile longitudinal reinforcement ratio, hoop tie ratio, shear span, and axial force. The six actual piers excluding the three scale specimens were all designed according to the Specifications for Steel Highway Bridges of 1965, and hence the hoop tie ratio is significantly low at 0.044 ~ 0.088%. On the other hand, the 1/3 scale specimens were constructed based on the 1990 standards with a hoop tie ratio of 0.33 ~ 0.34%. There is a report⁶⁾ saying that the shear crack inclination angle increases linearly with an increase in stirrup ratio based on simple beam test results.

As the nine piers differ in hoop tie ratio depending on which standards were used in their design, the focus was on hoop tie ratio in investigating the crack inclination angle. The relationship between shear crack inclination angle and hoop tie ratio is shown in Fig. 26. The experimental crack inclinations tended to increase with increasing hoop tie ratio, though there is some scatter

because the angles were merely the average of predominant cracks. The analytical values were in general smaller than the experimental values, but the same trend was also seen in the relationship between crack inclination angle and hoop tie ratio. When flexural shear failure or shear failure is anticipated, as in the case of actual RC piers with a small hoop tie ratio, the analytical crack inclination angle at the ultimate state is approximately 30° , which is considerably smaller than the 45° assumed in conventional truss theory. In contrast, in large-scale specimens having relatively large hoop tie ratios, the analytical crack inclination angle is substantially larger, at $55 \sim 60^\circ$, as compared with that of the actual bridge piers.

7.3 Relationship Between Maximum Shear Stress and Effective Height of concrete

Factors that are influential on the maximum shear stress of concrete include the effective depth of cross section, longitudinal tensile reinforcement ratio, axial force, and the shear span-effective depth ratio. As the effective depth of the cross section of the piers considered in the current investigation varied widely from 40 cm to 420 cm, this was taken as the factor of interest.

Analytical values indicating the relationship between maximum shear stress and effective depth of concrete are shown in Fig. 27, together with the experimental values. The maximum shear stress is the value derived by dividing the analytical maximum shear strength by the cross sectional area for shear resistance ($bw \cdot d$) of the concrete.

The maximum shear stress showed a tendency to fall with increasing effective depth. In particular, the maximum shear stress of specimens with an effective depth of less than 1 m was approximately 8.0 kg/cm^2 , a rather large value corresponding to nearly twice the maximum shear stress of actual piers.

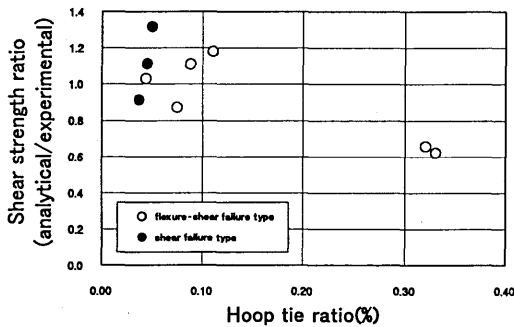


Fig. 28 Relationship between shear capacity ratio and hoop tie ratio

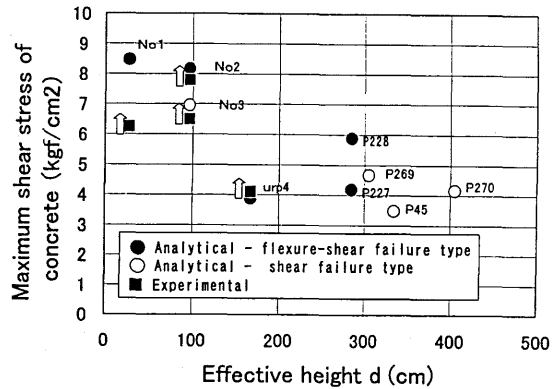


Fig. 27 V_c and V_s of concrete

7.4 Shear Strength ($V_c + V_s$)

The ultimate shear strength (a combination of the shear strengths of the concrete and the hoop ties at the ultimate state) derived from the Concrete Specifications and the Collins model were compared. In Fig. 28, the ordinate shows the ratio of analytical shear strength by the Concrete Specifications to that by the Collins model ("shear strength ratio"), and the abscissa shows the hoop tie ratio.

At small hoop tie ratios of $0.03 \sim 0.11\%$, the shear strength ratio was $0.9 \sim 1.3$, meaning that the shear strength given by the Concrete Specifications and the Collins model were roughly similar. In the ultimate stage, however, the concrete shear strength derived using the Collins model was smaller than that derived by the Concrete Specifications, while the shear strength of the hoop ties was greater than that given by the Concrete Specifications, whose basis is 45° truss theory, because the crack inclination angle is reduced at the ultimate state. As a result, in analysis by the Collins model, the extra shear strength provided by the hoop ties begins to supplement the shortfall in shear strength provided by the concrete, and accordingly the sum of the two is almost the same as that derived using the Concrete Specifications.

On the other hand, in piers with relatively large hoop tie ratios of 0.30 ~ 0.35%, the shear strength ratio by the Collins model was approximately 0.6, considerably smaller than that given by the Concrete Specifications, because no extra strength was added by the hoop ties since the crack inclination angle at the ultimate state was larger than 45°. If this type of pier is subjected to one-directional loading, its behavior tends to be governed by flexure and its ultimate state is rarely determined by the shear strength. Nevertheless, further investigation may be needed because the shear strength might be even lower if such a pier is subjected to reverse cyclic loading.

8. CONCLUSIONS

The mechanism of shear damage to RC piers was evaluated, both experimentally and analytically, using 1/3 scale specimens, an actual intact RC pier, and actual piers that suffered damage in the Hyogoken-Nanbu Earthquake. The following conclusions were drawn from the results:

- ① Concerning shear capacity, hoop tie stress, and crack inclination angle, analytical results obtained from 1/3 scale specimens and an actual intact pier utilizing the Modified Compression Field Theory (Collins model) showed relatively good agreement with the experimental results. Also, according to the analytical results, the shear resistance carried by the concrete in scale specimens and actual RC piers tended to decrease between yielding of the longitudinal reinforcement and the maximum loading.
- ② The range in which the shear resistance carried by the concrete declined was found to be governed by the principal tensile stress transferred via the shear crack plane. As this stress is apt to be influenced by the crack interval and crack width, a more detailed evaluation of this interaction may be needed.
- ③ In the analysis of 1/3 scale specimens, the hoop tie stress gradually increased with rising shear force, but in the experiment the stress increased slowly at first before suddenly rising around the ultimate state.
- ④ It was found from a parameter analysis using the Collins model that the crack inclination angle differs according to the hoop tie ratio, a tendency also observed in the experiments on scale specimens. In piers that suffered shear damage with a relatively large hoop tie ratio, the crack inclination angle was larger than the 45° in the experiments, but the analytical crack inclination angle was smaller than that derived by the Concrete Specifications, which presupposes yielding of hoop ties based on the truss model with diagonal member angle of 45°. However, in this case the web might undergo diagonal compressive failure prior to the hoop ties reaching the yielding point, so this type of failure mode also needs to be considered at the design stage. If such piers are subjected to one-directional loading, they tend to be governed by flexure and the ultimate state is rarely determined by shear strength. Nevertheless, further investigation may be needed because the shear strength might be yet lower if they are subjected to reverse cyclic loading even after serious deformation associated with yielding of the longitudinal reinforcement.

REFERENCES

- [1] Nakamura, H. and Higai, I., "Evaluation of Shear Strength of RC Beam Section Based on Extended Modified Compression Field Theory", Proc. of JSCE, V-23, No. 490, pp. 157-166, 1994.5 (in Japanese)
- [2] Vecchio, F.J. and Collins, M.P., "Predicting the Response of Reinforced Concrete Beams Subject to Shear Using Modified Compression Field Theory", ACI Structural Journal, pp. 258-268, 1998
- [3] Collins, M.P., Mitchell, D., *Prestressed Concrete Structures*, Prentice Hall, 1991
- [4] Priestley, M.J.N., Seible, F., and Calvi, G.M., *Seismic Design and Retrofit of Bridges*, John Wiley & Sons, Inc., 1996
- [5] Kosa, K., Kobayashi, K., Murayama, Y., and Yoshizawa, Y., "Experimental Study on Reversed Load-Displacement Behavior of RC Piers by Large Scale Model Tests", Proc. of JSCE, V-31, No. 538, pp. 47-56, 1996.5 (in Japanese)
- [6] Walraven, J., Uijl, J.D., and Al-Zubi, N., "Structural Lightweight Concrete: Recent Research", HERON, V-40, No.1, pp. 5-30, 1995